

Perfect anomalous transport of subdiffusive cargos by molecular motors in viscoelastic cytosol

Igor Goychuk^{1,*}

¹*Institute for Physics and Astronomy,
University of Potsdam,
Karl-Liebknecht-Str. 24/25,
14476 Potsdam-Golm,
Germany*

Multiple experiments show that various submicron particles such as magnetosomes, RNA messengers, viruses, and even much smaller nanoparticles such as globular proteins diffuse anomalously slow in viscoelastic cytosol of living cells. Hence, their sufficiently fast directional transport by molecular motors such as kinesins is crucial for the cell operation. It has been shown recently that the traditional flashing Brownian ratchet models of molecular motors are capable to describe both normal and anomalous transport of such subdiffusing cargos by molecular motors with a very high efficiency. This work elucidates further an important role of mechanochemical coupling in such an anomalous transport. It shows a natural emergence of a perfect subdiffusive ratchet regime due to allosteric effects, where the random rotations of a “catalytic wheel” at the heart of the motor operation become perfectly synchronized with the random stepping of a heavily loaded motor, so that only one ATP molecule is consumed at each motor step along microtubule on average. However, the number of rotations made by the catalytic engine and the traveling distance both scale sublinearly in time. Nevertheless, this anomalous transport can be very fast in absolute terms.

I. INTRODUCTION

Intracellular transport by molecular motors is crucial for a eukaryotic cell operation ((Nelson, 2003; Phillips et al., 2013; Pollard et al., 2008)). This is especially true in view of the recent discoveries ((Luby-Phelps, 2013)) that various nanoparticle probes ((Guigas et al., 2007; Saxton and Jacobson, 1997)), as well as naturally occurring biological nanoparticles such as proteins ((Banks and Fradin, 2005; Weigel et al., 2011; Weiss et al., 2004)), viruses ((Seisenberger et al., 2001)), RNA messengers ((Golding and Cox, 2006)), various endosomes and granulates ((Bruno et al., 2011; Caspi et al., 2002; Jeon et al., 2011; Tabei et al., 2013; Tolic-Norrelykke et al., 2004)), including artificial magnetosomes ((Robert et al., 2010)), and also lipids ((Jeon et al., 2012; Kneller et al., 2011)) subdiffuse either in membrane or in cytosol of living cells. This means that the mean-square distance covered by such particles scales sublinearly in time, $\langle \delta r^2(t) \rangle \sim 2D_\alpha t^\alpha / \Gamma(1 + \alpha)$, where α is a power law exponent of subdiffusion, $0 < \alpha < 1$, D_α is subdiffusion coefficient (within an effective 1d description), and $\Gamma(z)$ is familiar gamma-function. For example, magnetosomes of radius about $R = 300$ nm subdiffuse in intact cytosol of PC3 tumor cells with $\alpha \approx 0.4$, and $D_\alpha \approx 170 \text{ nm}^2/\text{s}^{0.4}$ like in (Goychuk, 2015; Goychuk et al., 2014b; Robert et al., 2010). To subdiffuse over the distance of $2R$, such an endosome would require about 2.705×10^7 seconds or about 313 days. Clearly a passive transport of such par-

ticles by subdiffusion on any significant distance within the cell is just impossible on any physiologically relevant time scale. However, some cells must solve the tasks such as e.g. delivery of ion channels in a transfer bag provided by an endosome on the distances which can be even meter long, as e.g. in axons of some neuronal cells ((Hirokawa and Takemura, 2005)). So, how can cells solve such tasks even using an active transport by such molecular motors as kinesins, if cytosol is a gel-like viscoelastic medium causing subdiffusion? In particular, can such a transport be normal, rather than anomalously slow, in the sense that the traveling distance along the cell’s microtubuli highways scales not sublinearly in time, $\langle \delta r(t) \rangle \sim t^{\alpha_{\text{eff}}}$, with some $\alpha \leq \alpha_{\text{eff}} < 1$, what is expected, but simply linearly with $\alpha_{\text{eff}} = 1$. Can such a transport be effective and sufficiently fast? And how? These are some challenging questions to be answered.

The simplest modeling of a molecular motor is to represent it by a constant pulling force F acting on a cargo, which, otherwise, thermally subdiffuses ((Caspi et al., 2002)), when it is not coupled to the motor. When the motor walks on microtubuli constituting a random transport network (kinesins), or it changes its walking direction at random along the same track (myosins), the motor action on its cargo can be modeled by a fluctuating, non-thermal random force $F(t)$ ((Bruno et al., 2009; Caspi et al., 2002)). In the absence of motors, thermal subdiffusion in viscoelastic media is described by a generalized Langevin equation or GLE ((Amblard et al., 1996; Mason and Weitz, 1995; Waigh, 2005)), with a memory friction and thermal random force obeying the thermal fluctuation dissipation theorem (FDT), (Kubo, 1966; Zwanzig,

* igoychuk@uni-potsdam.de

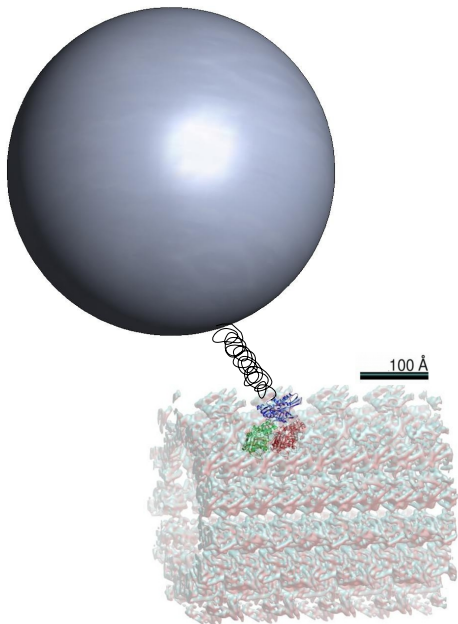


FIG. 1 Kinesin walking on microtubule and pulling cargo on an elastic tether.

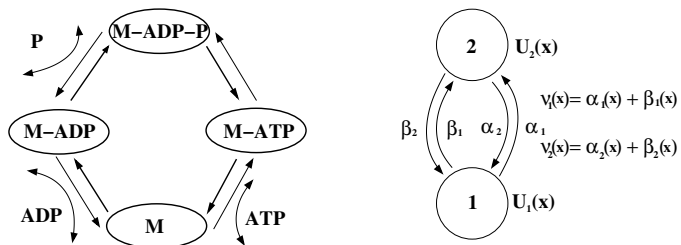


FIG. 2 More realistic biochemical cycle for one motor head (left) and the minimal two-state model of cycling (right) that includes a binding potential change due to a change of the charge state of the motor. Spatial dependence of the transition rates on the coordinate along a periodic polar background of microtubule provides an allosteric mechanism of the mechano-chemical coupling.

2001). An algebraically slow memory decay $\propto t^{-\alpha}$ yields subdiffusion $\langle \delta r^2(t) \rangle \sim t^{\alpha_{\text{eff}}}$, with $\alpha_{\text{eff}} = \alpha$, in the absence of non-thermal $F(t)$. The motor-driven diffusion has another exponent β , $\langle \delta r^2(t) \rangle \propto t^\beta$, with the maximal value $\beta_{\text{max}} = 2\alpha$ ((Bruno et al., 2009)) within this model. It can be superdiffusive only for $\alpha > 0.5$. However, an experiment by (Robert et al., 2010) in a medium with e.g. $\alpha = 0.4$ yielded $\beta = 1.3 \pm 0.1$ of active motor-assisted transport which is essentially larger than $2\alpha = 0.8$. Also another experiment by (Harrison et al., 2013) yielded $\beta \approx 1.74$ for the active transport with $\alpha \approx 0.58$ of the passive transport. Hence, such a modeling is far too sim-

ple and it cannot explain these experimental findings. A different modeling route of flashing Brownian ratchets ((Astumian and Bier, 1996; Jülicher et al., 1997; Parmegiani et al., 1999)) was taken by (Goychuk, 2015, 2016; Goychuk et al., 2014a,b). It is based on an extension of the previous research work on normal diffusion Brownian ratchets, see e.g. review by (Reimann, 2002), onto the case of viscoelastic subdiffusion featured by long-range memory correlations in the medium ((Goychuk, 2009, 2012b)). Such kind of subdiffusion naturally emerges in dense polymeric solutions, colloidal liquids and glasses, as well as cytosol of living cells ((Amblard et al., 1996; Gittes et al., 1997; Larson, 1999; Mason and Weitz, 1995; Pan et al., 2009; Santamaria-Holek et al., 2007; Waigh, 2005; Weiss, 2013)). A recent work ((Goychuk, 2017)) explains how this kind of subdiffusion can win over the medium's disorder also featuring such complex heterogeneous media as cytosol.

Rocking ratchets of normal diffusion ((Bartussek et al., 1994; Doering et al., 1994; Magnasco, 1993)) were generalized to viscoelastic subdiffusion by (Goychuk, 2010; Goychuk and Kharchenko, 2012, 2013; Kharchenko and Goychuk, 2013) and flashing ratchets ((Ajdari and Prost, 1992; Astumian and Bier, 1994; Prost et al., 1994; Rousselet et al., 1994)) by (Kharchenko and Goychuk, 2012). First application of flashing subdiffusive ratchets to molecular motors pulling nanocargos was done by (Goychuk et al., 2014a). In that work, motor and cargo make one subdiffusing quasi-particle in assumptions that a tether between them is infinitely rigid, and a spatially-asymmetric periodic ratchet potential acting on the motor stochastically switches between two realizations differing by a half of the spatial period shift, like in (Makhnovskii et al., 2004). Moreover, Markovian switching rates are identical and constant. Two such subsequent switches make one random cycle. The mechano-chemical coupling is neglected in that model. Depending on the size of cargo determining the subdiffusion coefficient of combined quasi-particle, frequency of the binding potential flashing, applied constant loading force, and other parameters, both anomalous and normal transport regimes can be realized, (Goychuk et al., 2014a). Very important is that the ratchet transport of a subdiffusive cargos can be perfectly normal, in the sense that each switching cycle results on average in the transport of motor with cargo on a distance of the spatial period, and the averaged number of such switches grows linearly in time (a perfect normal ratchet). However, anomalous transport regimes can also be readily enforced. This model provides a principal framework to explain the origin of $\beta = 1.3 \pm 0.1$ for $\alpha = 0.4$ in (Robert et al., 2010), and also origin of $\beta \approx 1.74$ in (Harrison et al., 2013) when the passive subdiffusion of lipid droplets with $\alpha \approx 0.58$ is changed to superdiffusion when they are actively transported by molecular motors.

The tether or linker between the motor and cargo is,

however, never infinitely rigid and the motor walking on microtubule is not fully exposed to viscoelastic constituents of cytosol. For this reason, (Goychuk et al., 2014b) considered a more involved model with the motor being normally diffusing in a ratchet potential of a similar kind (although, a different, saw-tooth form of the binding ratchet potential has been chosen), whereas the cargo is subdiffusing in viscoelastic cytosol, and both particles are connected by some elastic linker or tether, like in Fig. 1. Major earlier results were confirmed within this more realistic model, which still lacked, however, a mechano-chemical coupling between the mechanical motion of the motor and cargo and the biochemical cycling of the motor in its intrinsic conformational space. This drawback has been overcome by (Goychuk, 2015) who considered a very similar, in general features, model for the motor as one by (Astumian and Bier, 1996; Jülicher et al., 1997; Parmeggiani et al., 1999), which takes the mechano-chemical coupling into account, and also takes into account the fact that any tether must have a finite maximal extension length. The corresponding nonlinear effects can also be important, (Goychuk, 2015), for a weak tether like one in (Bruno et al., 2011). The model by (Astumian and Bier, 1996; Jülicher et al., 1997; Parmeggiani et al., 1999) is general and rich enough. It permits different specific models for the mechano-chemical coupling. One chosen by (Goychuk, 2015) (model A in this paper) allowed to closely reproduce the earlier results in (Goychuk et al., 2014b) for the same amplitude of the ratchet potential, $U_0 = 0.5 \text{ eV} = 20 k_B T_r$. In this particular case, the mechano-chemical coupling is effectively absent, and the motors perform cyclic turnovers with one almost fixed, position-independent rate for a very similar set of parameters as in the earlier work, (Goychuk et al., 2014b). However, already for $U_0 = 25 k_B T_r$ and $U_0 = 30 k_B T_r$ larger than the free energy of ATP hydrolysis, $\Delta G_{\text{ATP}} = 20 k_B T_r$, used to drive one biochemical cycle of the motor, the effects of mechano-chemical coupling become also very essential in the model A. The most striking effect is that the number of motor turnovers and the number of ATP molecules hydrolyzed during its operation start to scale sublinearly in time, $\langle N_{\text{turn}}(t) \rangle \propto t^\gamma$, with $\alpha_{\text{eff}} \leq \gamma \leq 1$. For the ratchet model with constant rates, $\gamma = 1$ always. Since the work against external loading force scales as $t^{\alpha_{\text{eff}}}$ and the energy consumed as t^γ , the thermodynamic efficiency generally decays in time as $1/t^\lambda$ with $\lambda = \gamma - \alpha_{\text{eff}}$, (Goychuk, 2015). However, it can be appreciably large, over 50% for a rather long time period (at the end of simulations corresponding to about 3 sec of physical time and traveling distances of the order of micrometer) at the maximum sub-power of operation ((Goychuk, 2015, 2016)). This regime requires, however, a large $U_0 > \Delta G_{\text{ATP}}$, with the stalling force essentially larger, about 10 pN (for $U_0 = 30 k_B T_r$, (Goychuk, 2015)) than 5 pN observed for kinesin by (Svoboda et al., 1993).

The major question we address in this work is whether

a similar regime is possible also for $U_0 = \Delta G_{\text{ATP}} = 20 k_B T_r$, and the stalling force in the range from 5 to 6 pN, as observed experimentally. It will be shown that such a regime indeed emerges, however, for a different model of mechano-chemical coupling (the model B below and in (Parmeggiani et al., 1999)) such that it cannot be reduced to a ratchet model with constant switching rates in a parameter range (like it happens within the model A). Moreover, the emergence of a perfect subdiffusive ratchet regime will be manifested with $\gamma = \alpha_{\text{eff}} < 1$, where thermodynamic efficiency does not decay in time. Such a perfect anomalous synchronization between anomalous biochemical turnovers of molecular motor and its mechanical motion due to a mechano-chemical coupling leads to a transport efficiency of nearly 100%, where consumption of one ATP molecule results into one step of the motor loaded with cargo along microtubule.

II. METHODS, THEORY AND SIMULATIONS

We consider a model based on one studied earlier ((Astumian and Bier, 1996; Goychuk et al., 2014a,b; Jülicher et al., 1997; Parmeggiani et al., 1999)). In essence, this is the same model as in (Goychuk, 2015). Molecular motor moves in a flashing periodic saw-tooth ratchet potential, $U(x + L, \zeta(t)) = U(x, \zeta(t))$, like one in the graphical abstract, with some potential height U_0 . Here, $L = 8 \text{ nm}$ is spatial period of microtubule, (Phillips et al., 2013; Pollard et al., 2008; Svoboda et al., 1993), and $\zeta(t)$ is a conformational state of the motor. Microtubuli are well-known to be a polar overall negatively charged periodic structures, (Baker et al., 2001), which provide transport highways for such motors as kinesins, (Pollard et al., 2008). Hence, emergence of a periodic and asymmetric potential for charged nanoparticles, like molecular motor-proteins attached to microtubule, is quite natural. Furthermore, ATP molecules which serve as the source of free energy for the motors like kinesins or myosins are also (negatively) charged, like are the products of the ATP hydrolysis: ADP and the phosphate group P_i . Thus, it is very natural that the binding potential flashes upon the conformational change of the motor related to its charge state fluctuations. The biochemistry of kinesin operation is very complex as it has two heads, with a simplest biochemical cycle depicted in the left part of Fig. 2. The simplest theoretical model for its cycling is given in the right part of Fig. 2 ((Astumian and Bier, 1996; Hill, 1989; Jülicher et al., 1997)): this is a biochemical two-cycle or bi-cycle, with some four lump rates. Of course, it presents a gross over-simplification, and hence, a truly minimal theoretical model. These rates are spatially-dependent, which expresses a mechano-chemical coupling, see below. In the spirit of this two-state model, one considers only two conformations, ζ_1 and ζ_2 , with

$\zeta(t)$ undergoing two-state fluctuations with spatially-dependent rates. Since two subsequent flashes make one cycle with the potential shifted by one spatial period, and the both motor heads are identical, it is natural to impose $U(x+L/2, \zeta_1) = U(x, \zeta_2)$ as an additional symmetry condition within this minimal model. Likewise, not only $\alpha_{1,2}(x+L) = \alpha_{1,2}(x)$, $\beta_{1,2}(x+L) = \beta_{1,2}(x)$, but also $\alpha_{1,2}(x+L/2) = \beta_{2,1}(x)$, etc. in this model. Furthermore, the energy ΔG_{ATP} is used to rotate the ‘‘catalytic wheel’’ ((Qian, 2005; Rozenbaum et al., 2004; Wyman, 1975)) in one preferred (counter-clockwise in Fig. 2) direction, which thermodynamically implies ((Hill, 1989; Qian, 2005))

$$\frac{\alpha_1(x)\beta_2(x)}{\alpha_2(x)\beta_1(x)} = \exp[\Delta G_{\text{ATP}}/(k_B T)], \quad (1)$$

for any x . This can be satisfied, e.g., by choosing

$$\begin{aligned} \frac{\alpha_1(x)}{\alpha_2(x)} &= \exp[(U_1(x) - U_2(x) + \Delta G_{\text{ATP}}/2)/(k_B T)], \\ \frac{\beta_1(x)}{\beta_2(x)} &= \exp[(U_1(x) - U_2(x) - \Delta G_{\text{ATP}}/2)/(k_B T)]. \end{aligned} \quad (2)$$

Furthermore, the total rates

$$\begin{aligned} \nu_1(x) &= \alpha_1(x) + \beta_1(x), \\ \nu_2(x) &= \alpha_2(x) + \beta_2(x) \end{aligned} \quad (3)$$

of the transitions between two energy profiles must satisfy

$$\frac{\nu_1(x)}{\nu_2(x)} = \exp[(U_1(x) - U_2(x))/(k_B T)] \quad (4)$$

at thermal equilibrium. This is condition of the thermal detailed balance, where the dissipative fluxes vanish both in the transport direction and within the conformational space of motor, at the same time ((Astumian and Bier, 1996; Jülicher et al., 1997)). It is obviously satisfied for $\Delta G_{\text{ATP}} \rightarrow 0$. There is still a lot of freedom in choosing rates, within the imposed requirements. One possibility is to choose $\alpha_1 = \beta_2 = \text{const}$. Then,

$$\begin{aligned} \nu_1(x) &= \alpha_1 \\ &+ \alpha_1 \exp[-(U_2(x) - U_1(x) + \Delta G_{\text{ATP}}/2)/(k_B T)], \\ \nu_2(x) &= \alpha_1 \exp[-(U_1(x) - U_2(x) + \Delta G_{\text{ATP}}/2)/(k_B T)] \\ &+ \alpha_1. \end{aligned} \quad (5)$$

This is our model A. Another choice with $\alpha_2 = \beta_1 = \text{const}$ and

$$\begin{aligned} \nu_1(x) &= \alpha_2 \\ &+ \alpha_2 \exp[(U_1(x) - U_2(x) + \Delta G_{\text{ATP}}/2)/(k_B T)], \\ \nu_2(x) &= \alpha_2 \exp[(U_2(x) - U_1(x) + \Delta G_{\text{ATP}}/2)/(k_B T)] \\ &+ \alpha_2. \end{aligned} \quad (6)$$

provides our model B, which is similar to the model B by (Parmeggiani et al., 1999). The difference between

the models A and B seems subtle. However, the results are rather different, see below. In particular, the mechano-chemical coupling is much stronger expressed in the model B.

The mechanical motion of the motor is mimicked by a Brownian particle subjected to the force $f(x, \zeta(t)) = -\partial U(x, \zeta(t))/\partial x$ coming from the binding potential, viscous friction force $-\eta_m \dot{x}$, and a thermal white Gaussian noise $\xi_m(t)$. The latter two are related by the second FDT, $\langle \xi_m(t)\xi_m(t') \rangle = 2k_B T \eta_m \delta(t-t')$ at the environmental temperature T . Inertial effects are neglected, like in the previous studies of molecular motors. Indeed, dynamics of nanoparticles in polymeric water solutions is typically overdamped. The inertial effects are present typically on the initial scales from picoseconds to nanoseconds, and we are interest in much longer times, up to seconds and minutes. Furthermore, the motor is assumed to be elastically coupled to a cargo (within a FENE model, (Goychuk, 2015; Herrchen and Öttinger, 1997)), with a spring constant κ_L and a maximal extension length r_{max} . The limit $r_{\text{max}} \rightarrow \infty$ corresponds to a harmonic linker. Moreover, it is generally subjected also to a constant loading force f_0 , which attempts to stop its directional motion being counter-directed. All in all, the motor is described by Eq. (7) in

$$\eta_m \dot{x} = f(x, \zeta(t)) - f_0 + \xi_m(t) + \frac{\kappa_L(y-x)}{1 - (y-x)^2/r_{\text{max}}^2}, \quad (7)$$

$$\begin{aligned} \eta_c \dot{y} &= - \int_0^t \eta_{\text{mem}}(t-t') \dot{y}(t') dt' - \frac{\kappa_L(y-x)}{1 - (y-x)^2/r_{\text{max}}^2} \\ &+ \xi_c(t) + \xi_{\text{mem}}(t). \end{aligned} \quad (8)$$

$f(x, \zeta(t))$ is piece-wise constant within the model considered. With the maximum of $U(x)$ dividing the potential period in the ratio $1 : p$, $p > 1$, it takes negative value $f_- = -(p+1)U_0/L$ within the spatial interval $[0, L/(p+1))$ and positive value $f_+ = (p+1)U_0/(pL)$ within the larger interval $[L/(p+1), L]$. Here, $U(0) = U(L) = 0$. If flashing is sufficiently slow, so that the particle has time to relax to the potential minimum after each potential flash it will be pushed forward by f_+ to a new potential minimum after a new flash. In this way, a perfect ratchet transport mechanism can be realized if flashing is not far too slow, so that the particle does not have enough time to escape to another potential minimum being thermally agitated (for a high potential barrier $U_0 \gg k_B T$ this is very seldomly the case). With increasing stopping force f_0 , the potential barrier diminishes and it vanishes at $f_{\text{st}} = f_+$, which is the stalling force in the absence of thermal fluctuations at $T = 0$. It must be mentioned in this respect that at physiological temperatures the stalling force depends strongly on temperature. To obtain it, U_0 should be replaced with a free energy barrier $U_0 \rightarrow F_0 = U_0 - TS$, with $S \approx 11.2 k_B$ for $\alpha_1 = 170 \text{ s}^{-1}$ within the model A, (Goychuk, 2015; Goychuk et al., 2014b). The entropic component is as

large as $T_r S \approx 11.2 k_B T_r$ at $T_r = 290$ K. Hence, to get a realistic stalling force for kinesin from 5 to 6 pN, (Svoboda et al., 1993), or about 7 pN ((Kojima et al., 1996)) at room temperatures, U_0 should be about $20 k_B T_r$, or somewhat larger. For $U_0 < 15 k_B T_r$, the above simple estimate does not work, cf. Fig. 6 in (Goychuk et al., 2014b), and the stalling force is far too small, as compare with the experimental values.

Also elastic coupling to the cargo will generally strongly affect the transport. The cargo motion is described by Eq. (9). It is subjected to both the viscous friction with friction coefficient η_c corresponding to about 80% of water content in cytosol, and to a viscoelastic memory friction characterized by the memory kernel $\eta_{\text{mem}}(t)$, which are related to the corresponding components of the thermal noise of the environment by the Kubo's second FDT, named also fluctuation-dissipation relation (FDR), (Kubo, 1966; Weiss, 1999; Zwanzig, 2001), $\langle \xi_c(t) \xi_c(t') \rangle = 2k_B T \eta_c \delta(t - t')$, $\langle \xi_{\text{mem}}(t) \xi_{\text{mem}}(t') \rangle = k_B T \eta_{\text{mem}}(|t - t'|)$. Viscoelasticity with a complex shear modulus $G^*(\omega) \propto (i\omega)^\alpha$ ((Larson, 1999; Mason and Weitz, 1995; Waigh, 2005)) corresponds to a strictly sub-Ohmic memory kernel, $\eta_{\text{mem}}(t) = \eta_\alpha t^{-\alpha} / \Gamma(1 - \alpha)$, $0 < \alpha < 1$, (Weiss, 1999), with fractional friction coefficient η_α , (Goychuk, 2009, 2012b). The corresponding memory term can be abbreviated as $\eta_\alpha d^\alpha y / dt^\alpha$ using the notion of fractional Caputo derivative ((Gorenflo and Mainardi, 1997; Mathai and Haubold, 2017)), and the corresponding thermal noise $\xi_{\text{mem}}(t)$ is fractional Gaussian noise (fGn), which is a time derivative of the fractional Brownian motion (fBm) by (Kolmogorov, 1940, 1991; Mandelbrot and van Ness, 1968). When the cargo is uncoupled to the motor ($\kappa_L = 0$), spread of its position variance is described by

$$\langle \delta y^2(t) \rangle = 2D_c t E_{1-\alpha, 2}(-[t/\tau_{\text{in}}]^{1-\alpha}), \quad (9)$$

(Kharchenko and Goychuk, 2013), where $E_{a,b}(z) = \sum_{n=0}^{\infty} z^n / \Gamma(an+b)$ is the generalized Mittag-Leffler function ((Mathai and Haubold, 2017)), and $D_c = k_B T / \eta_c$ is normal diffusion coefficient. Initially, at $t \ll \tau_{\text{in}} = (\eta_c / \eta_\alpha)^{1/(1-\alpha)}$ diffusion is normal, $\langle \delta y^2(t) \rangle \approx 2D_c t$ whereas at large times, $t \gg \tau_{\text{in}}$, it is anomalously slow, $\langle \delta y^2(t) \rangle \approx 2D_\alpha t^\alpha / \Gamma(1 + \alpha)$, with fractional diffusion coefficient D_α whose value plays a key role in anomalous transport processes.

A. Markovian embedding

Seen realistically, any power-law memory kernel has a long-time memory cutoff. Assuming it being exponential, $\eta_\alpha \rightarrow \eta_\alpha \exp(-\nu_h t)$, an effective friction coefficient $\eta_{\text{eff}} = \int_0^\infty \eta_{\text{mem}}(t) dt = \eta_\alpha \tau_{\text{max}}^{1-\alpha}$ can be introduced with $\tau_{\text{max}} = 1/\nu_h$. For $t \gg \tau_{\text{max}}$, diffusion will be again normal with the diffusion coefficient $D_{c,\text{eff}} = k_B T / (\eta_c + \eta_{\text{eff}})$. However, τ_{max} can be very large, in the range from tens

of seconds to hours, see e.g. Table I in (Goychuk, 2012a) (for a different model of memory cutoff). Furthermore, a small-time memory cutoff $\tau_{\text{min}} = 1/\nu_0$ must also always exist on physical grounds, in any realistic description of a condensed medium beyond the continuous medium approximation. Here, ν_0 is physically a maximal frequency of the mediums oscillators coupled to the Brownian particle within a dynamical theory of Brownian motion, (Weiss, 1999). Hence, it is natural to approximate a power-law scaling memory kernel between two memory cutoffs by a sum of exponentials,

$$\eta_{\text{mem}}(t) = \sum_{i=1}^N k_i \exp(-\nu_i t), \quad (10)$$

obeying fractal scaling $\nu_i = \nu_0 / b^{i-1}$, $k_i = C_\alpha(b) \eta_\alpha \nu_i^\alpha / \Gamma(1 - \alpha) \propto \nu_i^\alpha$, where $C_\alpha(b)$ is some constant, which depends on α and b , (Goychuk, 2009, 2012b; Hughes, 1995; Palmer et al., 1984) Obviously, $\tau_{\text{max}} = b^{N-1} / \nu_0$. Depending on b and α , the accuracy of approximation can be between 4% ($b = 10$, $\alpha = 0.5$) and 0.01% ($b = 2$, $\alpha = 0.5$), see in (Goychuk and Kharchenko, 2013). Upon use of the Prony series expansion (10), the non-Markovian dynamics of cargo allows for a multi-dimensional Markovian embedding, (Goychuk, 2012b), by introducing auxiliary Brownian quasi-particles mimicking viscoelastic modes of environment with coordinates y_i and frictional coefficients $\eta_i = k_i / \nu_i$:

$$\eta_c \dot{y} = -\frac{\kappa_L (y - x)}{1 - (y - x)^2 / r_{\text{max}}^2} - \sum_{i=1}^N k_i (y - y_i) \quad (11)$$

$$+ \sqrt{2\eta_c k_B T} \xi_0(t),$$

$$\eta_i \dot{y}_i = k_i (y - y_i) + \sqrt{2\eta_i k_B T} \xi_i(t), \quad (12)$$

where $\xi_i(t)$ are uncorrelated white Gaussian noises of unit intensity, $\langle \xi_i(t') \xi_j(t) \rangle = \delta_{ij} \delta(t - t')$, which are also uncorrelated with the white Gaussian noise sources $\xi_0(t)$ and $\xi_m(t)$. To have a complete equivalence with the stated GLE model in Eqs. (7), (9) with memory kernel (10), the initial positions $y_i(0)$ are sampled from independent Gaussian distributions centered around $y(0)$, $\langle y_i(0) \rangle = y(0)$ with variances $\langle [y_i(0) - y(0)]^2 \rangle = k_B T / k_i$, (Goychuk, 2012b). To see this equivalence, one has to (i) rewrite (12) in terms of viscoelastic force $u_i = k_i (y_i - y)$, (ii) formally solve the resulting equation for $u_i(t)$ with $\dot{y}(t)$ and $\xi_i(t)$ considered formally as some time-dependent functions and (iii) substitute the result, which consists of a regular part corresponding to friction with an exponentially decaying memory and a noise, into Eq. (11). Each noise component depends on $u_i(0)$, and all noise components are mutually independent. Considering $u_i(0)$ as random Gaussian variables with $\langle u_i(0) \rangle = 0$ and $\langle u_i^2(0) \rangle = k_i k_B T$, one can show that the resulting noise $\xi_{\text{mem}}(t)$ is indeed a wide sense stationary Gaussian stochastic process which satisfies FDR with the memory function (10), see in (Goychuk, 2009,

TABLE I Parameter sets

| Set, Model | $D_{0.4}$, $\text{nm}^2/\text{s}^{0.4}$ | α_2 , s^{-1} | α_1 , s^{-1} | U_0 , $k_B T_r$ | r_{rmax} , nm |
|---------------|---|---------------------------------|---------------------------------|----------------------|---------------------------|
| S_1, A | 171 | | 170 | 20 | ∞ |
| S_2, A | 1710 | | 170 | 20 | ∞ |
| S_5, A | 171 | | 34 | 20 | ∞ |
| S_7, A | 171 | | 170 | 25 | 80 |
| S_8, A | 171 | | 170 | 30 | 80 |
| S_9, A | 1710 | | 170 | 25 | 80 |
| S_{10}, A | 1710 | | 170 | 30 | 80 |
| S_1, B | 171 | 170 | | 20 | ∞ |
| S_2, B | 1710 | 170 | | 20 | ∞ |
| S_5, B | 1710 | 34 | | 20 | ∞ |
| S_6, B | 171 | 17 | | 20 | ∞ |
| S_7, B | 1710 | 17 | | 20 | ∞ |

2012b) for detail. The resulting $\xi_{\text{mem}}(t)$ presents a sum of independent Ornstein-Uhlenbeck processes which approximates fGn between two memory cutoffs. Langevin equations (7), (11), (12) considered together with a time-inhomogeneous Markovian process $\zeta(t)$, which is fully defined by two rates $\nu_{1,2}(x(t))$, provide a stochastic-dynamical description of the studied model. It is used in numerics.

B. Choice of parameters and the details of numerics

Like in (Goychuk, 2015; Goychuk et al., 2014b), we use $a_m = 100$ nm for the effective radius of kinesin, about 10 times larger than its linear geometrical size (without tether) in order to account for the enhanced effective viscosity experienced by the motor partially exposed to cytosol compared to its value in water. The viscous friction coefficient is estimated from the Stokes formula as $\eta_m = 6\pi a_m \zeta_w$, where $\zeta_w = 1$ mPa \cdot s is water viscosity used in calculations. Furthermore, the time is scaled in the units $\tau_m = L^2 \eta_m / U_0^*$ with $U_0^* = 10 k_B T_r$. For the above parameters, $\tau_m \approx 2.94$ μ s. Distance is scaled in units of L , elastic coupling constants in units of $U_0^* / L^2 \approx 0.64$ pN/nm, and forces in units of $U_0^* / L \approx 5.12$ pN. $\nu_0 = 100$ ($3.4 \cdot 10^7$ 1/s) was chosen which corresponds to $\tau_{\text{min}} = 29.4$ ns, and α was $\alpha = 0.4$, as found experimentally in (Bruno et al., 2011; Robert et al., 2010). Two cargo sizes were considered, large $a_c = 300$ nm, which corresponds to the magnetosome size in (Robert et al., 2010), and a ten times smaller one, like in Fig. 1. For larger cargo, we assume that its effective Stokes friction $\eta_c = 6\pi a_c \zeta_w$ is enhanced by the factor of $\eta_{\text{eff}} / \eta_c = 3 \cdot 10^4$ in cytosol. A particular embedding with $b = 10$ and $N = 10$ was chosen in accordance with our previous studies. With these parameters, $\tau_{\text{max}} = 10^9 \tau_{\text{min}} = 29.4$ s and fractional friction coefficient $\eta_\alpha = \eta_{\text{eff}} \tau_{\text{max}}^{\alpha-1} / r$ with $r \approx 0.93$, (Goychuk et al.,

2014b). The corresponding subdiffusion coefficient is $D_{0.4} = k_B T / \eta_{0.4} \sim 1.71 \cdot 10^{-16}$ $\text{m}^2/\text{s}^{0.4} = 171$ $\text{nm}^2/\text{s}^{0.4}$, in a semi-quantitative agreement with the experimental results in (Robert et al., 2010). Smaller cargo is characterized by $\eta_{\text{eff}} / \eta_c = 3 \cdot 10^3$ yielding $D_{0.4} = 1710$ $\text{nm}^2/\text{s}^{0.4}$, ten times larger. Furthermore, within the model A we used two values of the rate constant α_1 : 170 s^{-1} (fast) and 34 s^{-1} (slow), in order to match approximately the enzyme turnover rates $\nu \sim \alpha_1 / 2$ in Ref. (Goychuk et al., 2014b). Accordingly, we used mostly $U_0 = 20 k_B T_r$ in simulations, however, also two larger values of U_0 were used, see Table I, in order to arrive at the thermodynamic efficiencies larger than 50%. Within the model B we used three values of α_2 , see in Table I. The elastic spring constant is fixed to $\kappa_L = 0.32$ pN/nm in this paper. A similar value was found in experiment, (Kojima et al., 1996). For the maximal extension of linker we used $r_{\text{rmax}} = 80$ nm, (Pollard et al., 2008), and also $r_{\text{rmax}} = \infty$, which corresponds to harmonic linker in (Goychuk et al., 2014b). As it has been shown earlier in (Goychuk, 2015), for a strong linker considered, the harmonic approximation is, in principle, sufficient. Hence, within the model B in this paper we used only it. However, for weak linkers anharmonic effects can be very essential ((Goychuk, 2015)). Such weak linkers are not considered in this paper. The studied set of parameters is shown in Table I.

To numerically integrate stochastic Langevin dynamics for a fixed potential realization $U_{1,2}(x)$, we used stochastic Heun method implemented in parallel on NVIDIA Kepler graphical processors. Stochastic switching between two potential realizations is simulated using a well-known algorithm. Namely, if the motor is moving on $U_1(x)$ or $U_2(x)$ surface, at each integration time step δt it can switch with the probability $\nu_1(x)\delta t$ or $\nu_2(x)\delta t$, correspondingly, to another state, or to evolve further on the same potential surface. Here, $\nu_{1,2}(x)$ are the rates corresponding to either model A, or model B, see above. We used $\delta t = 5 \cdot 10^{-3}$ for the integration time step and $n = 10^3$ for the ensemble averaging. The maximal time range of integration was 10^6 , which corresponds to 2.94 sec of motor operation. Notice that a further increase of N does not influence results, whereas it exponentially increases η_{eff} for cargos. This means that η_α and D_α are the truly relevant parameters of fractional transport, and not η_{eff} . Furthermore, $\Delta G_{\text{ATP}} = 20 k_B T_r$ was taken in all numerical simulations, and $T = T_r = 290$ K, so that $k_B T_r \approx 25$ meV.

C. Stochastic energetics

Stochastic energetics can be considered following (Goychuk, 2015; Jülicher et al., 1997). The useful work done by motor against a loading force f_0 is $W_{\text{use}}(t) = f_0 \langle \delta x(t) \rangle \propto t^{\alpha_{\text{eff}}}$, whereas the input energy that it consumes scales as $W_{\text{use}}(t) = \Delta G_{\text{ATP}} \langle N_{\text{turn}}(t) \rangle$, where

TABLE II Parameters of the fit $R_{\text{th}}(f_0) = k(f_0/f_{\text{st}})[1 - (f_0/f_{\text{st}})^a]$, and the corresponding values of $R_{\text{th}}^{(\text{max})}$, and f_{max}

| Set, Model | k | f_{st} , pN | a | $R_{\text{th}}^{(\text{max})}$ | f_{max} , pN |
|--------------|--------|----------------------|-------|--------------------------------|-----------------------|
| S_1 , A | 0.385 | 6.00 | 1.112 | 0.103 | 3.06 |
| S_2 , A | 0.418 | 5.91 | 4.925 | 0.242 | 4.12 |
| S_5 , A | 0.454 | 4.79 | 2.405 | 0.192 | 2.88 |
| S_7 , A | 0.758 | 9.00 | 1.94 | 0.287 | 5.16 |
| S_8 , A | 0.909 | 10.00 | 20.08 | 0.744 | 8.59 |
| S_9 , A | 0.847 | 9.00 | 8.93 | 0.589 | 6.96 |
| S_{10} , A | 0.952 | 10.00 | 52.26 | 0.866 | 9.27 |
| S_1 , B | 0.4193 | 6.282 | 0.982 | 0.104 | 3.13 |
| S_2 , B | 0.615 | 6.24 | 3.865 | 0.324 | 4.14 |
| S_5 , B | 0.522 | 5.36 | 4.746 | 0.298 | 3.71 |
| S_6 , B | 0.493 | 5.01 | 2.148 | 0.197 | 2.94 |
| S_7 , B | 0.489 | 5.01 | 4.619 | 0.277 | 3.45 |

$\langle N_{\text{turn}}(t) \rangle \propto t^\gamma$ is the number of turnovers $1 \rightarrow 2 \rightarrow 1$. This yields for thermodynamic efficiency

$$R_{\text{th}}(t) = \frac{W_{\text{use}}(t)}{\Delta G_{\text{ATP}} \langle N_{\text{turn}}(t) \rangle} \propto 1/t^{\gamma - \alpha_{\text{eff}}}. \quad (13)$$

This definition is, however, not quite precise because it assumes that all the turnovers of the ‘‘catalytic wheel’’ occur with ATP hydrolysis. However, some turnovers occur backwards, with ATP synthesis, within this model. Since such backward turnovers occur seldomly for $\Delta G_{\text{ATP}} = 0.5$ eV, Eq. (13) only slightly underestimates the proper efficiency, see in (Goychuk, 2015). To correctly calculate consumption of ATP molecules one should count $p_1 \Delta G_{\text{ATP}}/2$, with $p_1 = (\alpha_1 - \beta_1)/(\alpha_1 + \beta_1)$ for the transition $U_1 \rightarrow U_2$, and $p_2 \Delta G_{\text{ATP}}/2$ with $p_2 = (\beta_2 - \alpha_2)/(\alpha_2 + \beta_2)$ for the transition $U_2 \rightarrow U_1$. A corresponding modification of (13) will be named the proper efficiency.

III. RESULTS

We first made a comparative study of the dependence of the transport exponent α_{eff} and thermodynamic efficiency on the loading force f_0 for two sets of parameters, S_1 and S_2 , within the models A and B, see in Fig. 3. For the larger cargo, the set S_1 , see in Table I, the results do not differ much: α_{eff} is around 0.6, which can explain $\beta = 1.3 \pm 1$ in (Robert et al., 2010). The maximal efficiency is about 10% and the stalling force is slightly larger in the model B, $f_{\text{st}} = 6.282$ pN, *vs.* $f_{\text{st}} = 6$ pN in the model A, see in Table II. The numerical data on the efficiency are parametrized in this paper by the dependence, (Goychuk, 2016),

$$R_{\text{th}}(f_0) = k \frac{f_0}{f_{\text{st}}} \left[1 - \left(\frac{f_0}{f_{\text{st}}} \right)^a \right], \quad (14)$$

TABLE III Power law exponents depending on the loading force f_0 , the case S_2 , model B

| f_0 , pN | α_{eff} | γ | λ |
|------------|-----------------------|----------|-----------|
| 0 | 0.854231 | 0.856338 | 0.002107 |
| 0.512 | 0.863078 | 0.865964 | 0.002886 |
| 1.024 | 0.872694 | 0.877308 | 0.004614 |
| 1.536 | 0.882037 | 0.888624 | 0.006587 |
| 2.048 | 0.890468 | 0.900774 | 0.010306 |
| 2.560 | 0.898387 | 0.914309 | 0.015922 |
| 3.072 | 0.900635 | 0.926184 | 0.025549 |
| 3.584 | 0.900195 | 0.940803 | 0.040608 |
| 4.096 | 0.900237 | 0.964067 | 0.063830 |
| 4.608 | 0.892551 | 0.988937 | 0.096386 |
| 5.120 | 0.890468 | 1 | 0.109532 |
| 5.632 | 0.839736 | 1 | 0.160264 |
| 6.148 | 0.807682 | 1 | 0.192318 |

TABLE IV Power law exponents depending on the loading force f_0 , the case S_6 , model B

| f_0 , pN | α_{eff} | γ | λ |
|------------|-----------------------|----------|-----------|
| 0 | 0.778586 | 0.799655 | 0.021069 |
| 0.512 | 0.792495 | 0.823397 | 0.030902 |
| 1.536 | 0.798144 | 0.868486 | 0.070342 |
| 2.048 | 0.799791 | 0.899897 | 0.100106 |
| 2.560 | 0.793568 | 0.937876 | 0.144308 |
| 3.072 | 0.78149 | 0.973073 | 0.191583 |
| 3.584 | 0.760739 | 1 | 0.239261 |
| 4.096 | 0.72811 | 1 | 0.27189 |
| 4.608 | 0.699885 | 1 | 0.300115 |
| 5.120 | 0.687050 | 1 | 0.312950 |

TABLE V Power law exponents depending on the loading force f_0 , the case S_5 , model A

| f_0 , pN | α_{eff} | γ | λ |
|------------|-----------------------|----------|-----------|
| 0 | 0.995152 | 1.00 | 0.004848 |
| 0.512 | 0.991188 | 1.00 | 0.008812 |
| 1.024 | 0.982147 | 1.00 | 0.017853 |
| 1.536 | 0.969404 | 1.00 | 0.030596 |
| 2.048 | 0.925052 | 1.00 | 0.074948 |
| 2.560 | 0.909704 | 1.00 | 0.090296 |
| 3.072 | 0.813889 | 1.00 | 0.186111 |
| 3.584 | 0.756685 | 1.00 | 0.243315 |
| 4.096 | 0.697763 | 1.00 | 0.302237 |
| 4.608 | 0.618159 | 1.00 | 0.381841 |

where k , a and f_{st} are considered as fitting parameters with their values given in Table II. It is derived from the assumptions that subvelocity v_α , defined by $\langle \delta x(t) \rangle = v_\alpha t^\alpha / \Gamma(1 + \alpha)$ with $\alpha = \alpha_{\text{eff}}$ decays with f_0 as $v_\alpha(f_0) = v_\alpha(0)[1 - (f_0/f_{\text{st}})^a]$, and $W_{\text{use}}(t)$ does not depend on f_0 . If these assumptions are justified, the

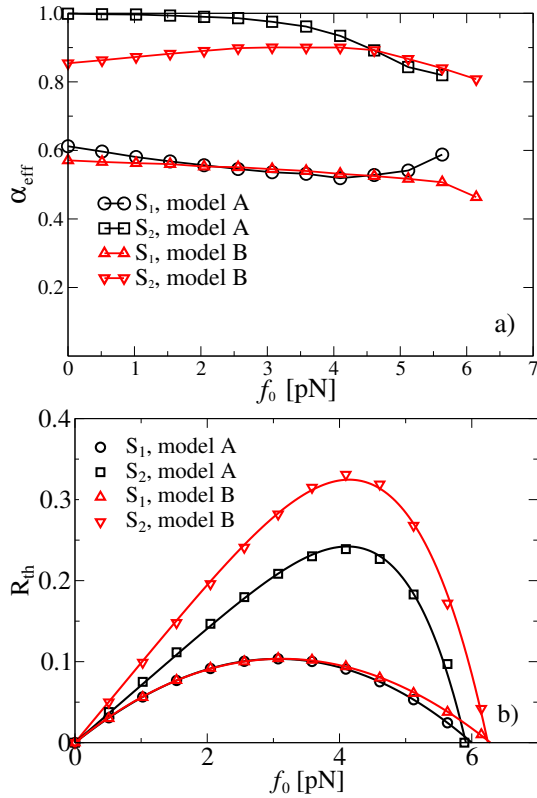


FIG. 3 (Color online). (a) Transport power exponent α_{eff} and (b) thermodynamic efficiency for the sets $S_{1,2}$ in the models A and B vs. loading force f_0 . Notice that in the case S_2 the motor has an essentially larger efficiency within the model B than the model A, although the transport is more anomalous within the model B, especially for a small load. In part (b), full lines present fits with Eq. (14) with parameters shown in Table II. Thermodynamic efficiency is calculated in accordance with Eq. (13) at the end point of simulations.

TABLE VI Power law exponents depending on the loading force f_0 , the case S_5 , model B

| f_0 , pN | α_{eff} | γ | λ |
|------------|-----------------------|----------|-----------|
| 0 | 0.928004 | 0.928294 | 0.000290 |
| 0.512 | 0.937161 | 0.937699 | 0.000538 |
| 1.024 | 0.945399 | 0.946257 | 0.000858 |
| 1.536 | 0.950206 | 0.952371 | 0.002165 |
| 2.048 | 0.952820 | 0.956787 | 0.003967 |
| 2.560 | 0.956454 | 0.963371 | 0.006917 |
| 3.072 | 0.957644 | 0.970018 | 0.012374 |
| 3.584 | 0.956840 | 0.978205 | 0.021365 |
| 4.096 | 0.954589 | 0.989856 | 0.035267 |
| 4.608 | 0.938140 | 0.999875 | 0.061735 |
| 5.120 | 0.917003 | 1.00 | 0.082997 |

maximum of R_{th} in Eq. (14), $R_{\text{th}}^{(\text{max})} = ka/(1+a)^{1+1/a}$ at $f_{\text{max}} = f_{\text{st}}/(1+a)^{1/a}$, corresponds to thermodynamic efficiency at the maximum of sub-power. Whereas the latter assumption is well fulfilled within the model A at

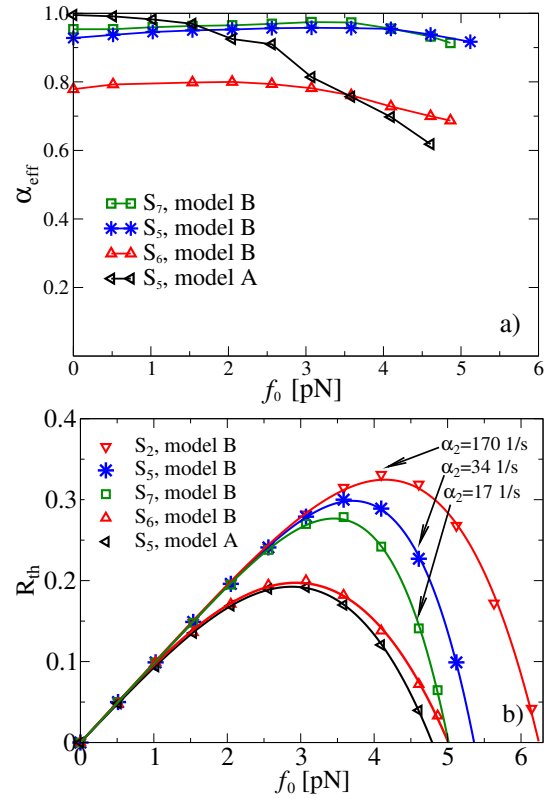


FIG. 4 (Color online). (a) Transport power exponent α_{eff} and (b) thermodynamic efficiency vs. loading force f_0 for several other sets shown in the plots and discussed in the text. In part (b), full lines present fits with Eq. (14) and parameters shown in Table II. Thermodynamic efficiency is calculated in accordance with Eq. (13).

$U_0 = 20 k_B T_r$, (Goychuk, 2015), generally it is not correct, especially within the model B, see below, where the ATP consumption generally strongly depends on f_0 . Hence, the maximum of the fit (14) not always correspond to the maximum at maximal sub-power, see below. Nevertheless, it works nicely anyway. Its relation to Jacobi efficiency in the linear operation regime of normal motors should also be mentioned. Indeed, it reduces to Jacobi efficiency, at $a = 1$ and $k = 1$, (Goychuk, 2016), and $\alpha_{\text{eff}} = \gamma = 1$.

For a smaller cargo, sets S_2 , the distinction between the models A and B becomes quite evident in Fig. 3. First, in the model A, α_{eff} starts from $\alpha_{\text{eff}} \approx 1$ at small f_0 , and then it monotonously declines to about 0.8 at the stalling force. In the model B, $\alpha_{\text{eff}} \approx 0.854$ at $f_0 = 0$, see in the Table III. It increases with f_0 to about 0.90 at f_0 corresponding to the maximum of thermodynamic efficiency. After this, it declines to about 0.808 at the stalling force, which is slightly larger than one within the model A.

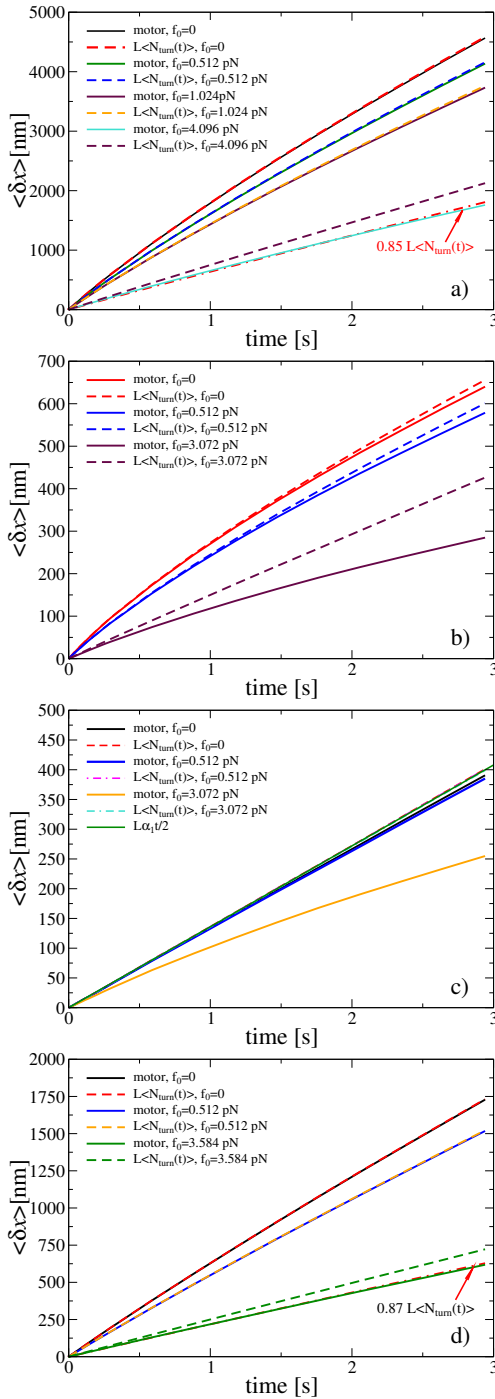


FIG. 5 (color online). Mean motor displacement $\langle \delta x(t) \rangle$ and $L\langle N_{\text{turn}}(t) \rangle$ vs. time for several values of f_0 shown in the plots for the sets: (a) S_2 , model B; (b) S_6 , model B; (c) S_5 , model A; (d) S_5 , model B. Good agreement between $\langle \delta x(t) \rangle$ and $L\langle N_{\text{turn}}(t) \rangle$ reflects a perfect anomalous synchronization between stochastic turnovers of catalytic wheel and the motor stepping along microtubule. For small f_0 in the parts (a) and (d), increase of f_0 results in a synchronous slowing down of both the biochemical turnovers and the processive mechanical motion. It corresponds to a perfect anomalous ratchet regime. Even at the load corresponding to maximal thermodynamic efficiency in the cases (a) and (d), only about 15% and 13%, correspondingly, of ATP molecules consumed do not result into a perfect transport event – promotion on the length L along microtubule. In part (c), $\langle N_{\text{turn}}(t) \rangle$ practically does not depend on f_0 and is well described by $\alpha_1 t/2$.

1. Perfect subdiffusive ratchet

Within the model A, at small f_0 our motor realizes a perfect normal ratchet transport, where stochastic stepping along microtubule is perfectly synchronized with the normal turnovers of the catalytic wheel characterized by a turnover frequency equal to the half of the flashing frequency, (Goychuk, 2015; Goychuk et al., 2014b). A strikingly new result within the model B is that our ratchet realizes a perfect subtransport, with anomalous turnovers of catalytic wheel which cannot be characterized anymore by a normal turnover frequency. Rather, one must introduce a new notion, the enzyme catalytic sub-velocity ω_γ by $\langle N_{\text{turn}}(t) \rangle = \omega_\gamma t^\gamma / \Gamma(1 + \gamma)$. As Fig. 5, a and Table III reveal, for small f_0 , $\alpha_{\text{eff}} \approx \gamma < 1$, and $\lambda \approx 0$. We are dealing with a perfect subdiffusive ratchet, where due to a mechano-chemical coupling, the consumption of ATP molecules by the motor scales sublinearly with time, and nevertheless the transport is perfect in the sense that consumption of one ATP molecule leads to one step. Indeed, in Fig. 5, a, $\langle \delta x(t) \rangle$ almost coincides with $L\langle N_{\text{turn}}(t) \rangle$ for $f_0 = 0.512$ pN and $f_0 = 1.024$ pN. Even for $f_0 = 4.096$ pN near to R_{th} maximum, $\langle \delta x(t) \rangle \approx 0.85L\langle N_{\text{turn}}(t) \rangle$, which means that only about 15% of biochemical turnovers do not lead to a successful step over L . $R_{\text{th}} \approx 0.324$ at this maximum is much larger than in the model A, for small cargo, see in Fig. 3, a, and subdiffusive transport is very fast in absolute terms, cf. Fig. 5, a. Notice, that very differently from the model A, see in Fig. 5, c, the consumption of ATP molecules strongly depend on f_0 within the model B: it is smaller for larger f_0 (until about f_{max}). This is a very important feature of the perfect subdiffusive ratchet mechanism.

The transport of the large cargo is far from being perfect in the case S_1 , model B. However, maybe its quality can be drastically improved at smaller operational frequencies of the motor? Indeed, this is the case, as Fig. 4, and Fig. 5, b, reveal for the set S_6 , model B. For a smaller $\alpha_2 = 34 \text{ s}^{-1}$, α_{eff} increases at $f_0 = 0$ from about 0.6 (for $\alpha_2 = 170 \text{ s}^{-1}$) to about 0.8, see in the Table IV, and the maximum of R_{th} increases to about 0.2, see in Fig. 4, b, i.e. it almost doubles, cf. Table II. Even if the quality of anomalous synchronization is somewhat worse in this case than in the case S_2, B of smaller cargo, it is, nevertheless, quite impressive: a heavily loaded motor can walk over the distance of 650 nm at $f_0 = 0$ (which is normal operational regime of linear molecular motors in living cells) within the less than 3 sec, see in Fig. 5, b. Within the model A, transport of large cargo shares similar features for the parameter set S_5 , with respect to thermodynamic efficiency, see in Fig. 4, b. However, the dependence of the transport exponent α_{eff} on f_0 is entirely different. First, it features an almost normal transport at small f_0 , cf. 4, a. It occurs in a perfect normal ratchet regime, see in Fig. 5, c. Second, the turnover frequency of the enzyme practically does not depend on

f_0 , see in Fig. 5, c. It is equal to $\alpha_1/2$. Hence, with the increase of the static load f_0 strength, at the maximum of R_{th} , α_{eff} drops to about 0.81, see in Table V and Fig. 4, while γ remains one. This leads to a substantial decay of $R_{\text{th}} \propto 1/t^\lambda$ in time, with $\lambda \approx 0.186$. Although, within the model B, set S_6 , the decay of the maximum of R_{th} has about the same $\lambda \approx 0.196$, see in Table IV at $f_0 = 3.072$ pN. This is so because in this case γ arrives at the value of one. Hence, also in this respect, the models A and B are similar. However, once again, the stalling force is slightly larger in the model B.

2. Role of the rate α_2

Next, it is interesting to clarify the influence of the rate α_2 , which is determined, in particular, by the ATP concentration ((Astumian and Bier, 1996; Jülicher et al., 1997; Parmeggiani et al., 1999)), on the transport properties within the model B. In fact, the sets S_2 , S_5 , and S_7 differ only by the value of α_2 . Fig. 4, b shows that the smaller is α_2 , the smaller is the maximum of thermodynamic efficiency, and the smaller is the stalling force. However, at the same time, smaller α_2 corresponds to larger α_{eff} , see in Fig. 4, a, i.e. transport becomes closer to normal. Within the model B, the behavior of α_{eff} versus f_0 displays one and the same universal feature: first, it slightly increases arriving at a maximum, and then it slightly drops. α_{eff} is generally much less sensitive to f_0 within the model B, as compare with the model A. This is because within the model B the mechano-chemical coupling adjusts the tempo of biochemical cycling in response to f_0 . It becomes slower. Fig.5, d and Table VI demonstrate this effect for the set S_5 , B. Once again, an almost perfect subdiffusive ratchet is realized for a sufficiently small cargo. At $f_0 = 3.584$ pN, which corresponds to the maximum of R_{th} of about 30%, only about 13% of the motor turnovers are futile, not resulting in a successful step along microtubule. A power-stroke like, mechano-chemically adaptive mechanism can lead to a perfect, energetically efficient subtransport.

3. Thermodynamic efficiency over 50%

Within the model A, the mechano-chemical coupling becomes also very essential, however, for a larger U_0 . Then, thermodynamic efficiency can overcome 50%, even at the maximum of sub-power. Figs. 6, 7 demonstrate this striking effect. For the set S_{10} , thermodynamic efficiency exceeds 80% at its maximum, cf. Fig. 6. The maximum of R_{th} vs. f_0 in this case does not corresponds to thermodynamic efficiency at the maximum of sub-power $P_\alpha(f_0) = v_\alpha(f_0)f_0$ because of a strong mechano-chemical coupling. Nevertheless, the maximum of the latter one takes place at $f_0 = 7.168$ pN in Fig. 7, which corresponds

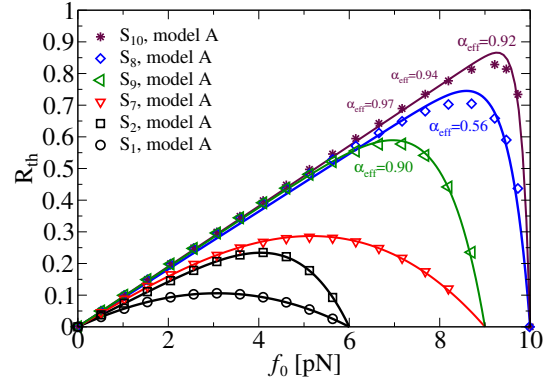


FIG. 6 (Color online) Thermodynamic efficiency vs. loading force within model A for $U_0 = 25 k_B T_r$ and $U_0 = 30 k_B T_r$, as compare with the cases $S_{1,2}$, corresponding to $U_0 = 20 k_B T_r$. Full lines present fits with Eq. (14) with parameters shown in Table II. Notice a substantial increase of efficiency for larger U_0 . It can exceed 80% in the case S_{10} . Here, numerical data present the results on the proper thermodynamic efficiency as described in the text. It is slightly larger than one in Eq. (13), see Fig. 6 in (Goychuk, 2015) and the corresponding discussion therein for detail.

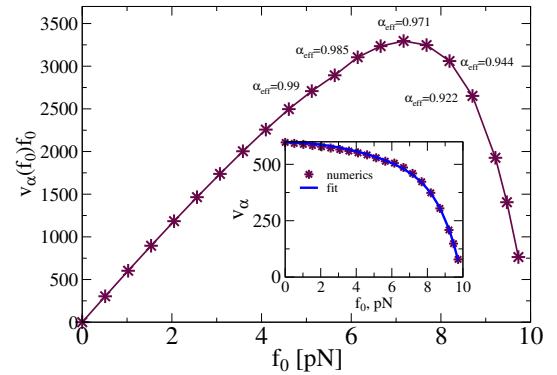


FIG. 7 (Color online). Subpower $v_\alpha(f_0)f_0$ (in the units of $\text{pN} \cdot \text{nm}/\text{s}^{\alpha_{\text{eff}}}$) and subvelocity (inset, in the units of $\text{nm}/\text{s}^{\alpha_{\text{eff}}}$) versus loading force, in the units of pN, for the set S_{10} , model A. $\alpha_{\text{eff}} \approx 1$ for $f_0 < 5$ pN. Several other values are shown in the plot. At the maximum of subpower, at $f_0 = 7.168$, $\alpha_{\text{eff}} \approx 0.9712$, and $\gamma \approx 0.9708$. Hence, the motor operates as a perfect subdiffusive ratchet whose thermodynamic efficiency at the subpower maximum is about 70%, in accordance with Fig. 6. The numerical data in inset are fitted by the dependence $v_\alpha(f_0) = v_1(0) [1 - (f_0/f_1)^2 - (f_0/f_2)^{a_2}]$, with $v_1(0) = 597.12$ nm/s, $f_1 = 15.60$ pN, $f_2 = 10.52$ pN, and $a_2 = 9.258$.

approximately to impressive 70% in Fig. 6. Hence, we provided an instance of anomalous motor whose efficiency at maximal sub-power essentially exceeds 50%. This is a seminal result. Very interesting is also dependence of the motor (sub)velocity of f_0 in this case. For small f_0 it is approximately quadratic, $v_\alpha(f_0) \approx v_1(0)[1 - (f_0/f_1)^2]$, see inset in Fig. 7. This is very different from the low efficient quasi-linear regime, where it is nearly linear, (Goychuk et al., 2014a,b).

IV. DISCUSSION

The model B exhibits a much stronger mechano-chemical coupling than the model A. Within this model, mechano-chemical coupling is very essential already for $U_0 = 20 k_B T_r$, which is a reasonable choice for kinesins II, given a typical stalling force of these motors. While the transport of a large cargo, like magnetosomes in (Robert et al., 2010), looks very similar in both models, for a fast operating motor, the transport of smaller cargos is always profoundly different. The differences are also seen for slowly operating motors. Transport of the large cargo in this paper is characterized for $\alpha_2 = 170 \text{ s}^{-1}$ by a transport exponent around $\alpha_{\text{eff}} = 0.6$ for $\alpha = 0.4$, which can easily explain the observed superdiffusion exponents around $\beta = 1.3 \pm 0.1$ in the experiment, (Robert et al., 2010). Energetically, such a transport is, however, inefficient. Nevertheless, while operating slower the motors can realize also energetically very efficient transport in viscoelastic cytosol. Indeed, with a tenfold reduction of α_2 from 170 s^{-1} to 17 s^{-1} , such a near-to-perfect anomalous ratchet regime is realized for $f_0 = 0$ within the model B (set S_6) with α_{eff} increased to about 0.8. It should be noticed in this respect that normal *modus operandi* of linear motors like kinesin in living cells is one at zero thermodynamic efficiency. Indeed, the chemical potential of neither motor, nor cargo is typically increased. This is very different from the work of e.g. ionic pumps which must energize ions by transferring them against a corresponding electrochemical gradient. For pumps, namely thermodynamic efficiency is of paramount importance and must be optimized. Nevertheless, the ability to sustain substantial constant forces f_0 is important for a strong and good motor. It can be checked e.g. in the experiments with optical tweezers. Within the model B, the motor adapts its biochemical cycling to the increased f_0 . It cycles slower and anomalously, while within the model A it cycles normally and at the same nearly constant tempo for $U_0 = 20 k_B T_r$. This advantage of the model B is clearly seen for smaller cargos, where this study revealed a perfect and fast (in absolute terms) anomalous ratchet regime. The motor adapts its cyclic sub-velocity, and even at the maximum of thermodynamic efficiency, while working also against a strong f_0 , the portion of the futile (in the transport sense) turnovers can be really small, just from 13% to 15%. This is definitely provides some benefits with respect to energetic costs of transport.

The mechano-chemical adaptation becomes also relevant within the model A, however, for larger U_0 . We showed that for $U_0 = 0.75 \text{ eV}$ thermodynamic efficiency of our model motor can exceed 80% within an almost perfect anomalous ratchet regime while transferring smaller cargo against a large bias of $f_0 = 9 \text{ pN}$ with $\alpha_{\text{eff}} \approx \gamma \approx 0.92$. Also efficiency at maximum sub-power can reach impressive 70% at $f_0 \approx 7.2 \text{ pN}$ with $\alpha_{\text{eff}} \approx \gamma \approx 0.97$. In such a thermodynamically highly efficient regime, the

motor (sub)-velocity declines quadratically with f_0 at small loading forces. Such a regime does not seem, however, to be relevant for real kinesins whose velocity in experiments decline linearly with loading force, see in (Kojima et al., 1996; Svoboda et al., 1993). Nevertheless, its existence is very inspiring, especially when one thinks about perspectives of an optimal motor design, (Cheng et al., 2015; Goychuk, 2016). Clearly, a highly efficient operation is possible also in highly dissipative viscoelastic media like cytosol, as our study convincingly shows. This removes mental barriers and opens great perspectives for an optimal design of artificial molecular motors, (Cheng et al., 2015; Erbas-Cakmak et al., 2015), especially in allowing to avoid some common fallacy traps, (Goychuk, 2016).

Notice, that within the both studied models of mechano-chemical coupling, we assumed either α_1 , or α_2 be spatially-independent constants. Allosteric effects are nevertheless present because other rates are spatially dependent. They can be made stronger, when e.g. α_1 in the model A is different from zero only in a small domain around the potential minimum. Strong allosteric effects are presumably very important for operating natural molecular motors and for designing the new ones, (Cheng et al., 2015). Such effects can be used for a further optimization of the motor performance, which is very high already in the current, simplified and non-optimized version.

V. CONCLUSIONS

To conclude, in this paper we extended our previous studies of anomalous transport of subdiffusing cargos by molecular motors in viscoelastic cytosol of living cells and showed the emergence of a perfect subdiffusive ratchet regime due to a mechano-chemical coupling. This anomalous transport regime is characterized by anomalously slow biochemical cycling of molecular motors accompanied by a sublinear consumption of ATP molecules in time, with their optimal use: consumption of one ATP molecule results on one step over the spatial period of microtubule. Moreover, such a transport can be very fast in absolute terms, not bringing some disadvantages in this respect. Such anomalous transport regimes can be very important in the economics of living cells. Their assumed presence provides a true challenge for the experimentalists to reveal. The author hope and expect that the theoretical prediction of a slow consumption of ATP molecules by molecular motors, which cannot be characterized by a rate, while transporting efficiently various cargos within interior of living cells will eventually be confirmed experimentally.

ACKNOWLEDGMENT

Funding of this research by the Deutsche Forschungsgemeinschaft (German Research Foundation), Grant GO 2052/3-1 is gratefully acknowledged.

REFERENCES

- Ajdari, A. and Prost, J.: 1992, Mouvement induit par un potentiel p eriodique de basse sym etrie: di electrophorese puls ee, *Comp. Rend Acad. Sci., Paris II* **315**, 1635–1639.
- Amblard, F., Maggs, A. C., Yurke, B., Pargellis, A. N. and Leibler, S.: 1996, Subdiffusion and anomalous local viscoelasticity in actin networks, *Phys. Rev. Lett.* **77**, 4470–4473.
- Astumian, R. D. and Bier, M.: 1994, Fluctuation driven ratchets: Molecular motors, *Phys. Rev. Lett.* **72**, 1766–1769.
- Astumian, R. D. and Bier, M.: 1996, Mechanochemical coupling of the motion of molecular motors to atp hydrolysis, *Biophys. J.* **70**, 637.
- Baker, N. A., Sept, D., Joseph, S., Holst, M. J. and McCammon, J. A.: 2001, Electrostatics of nanosystems: Application to microtubules and the ribosome, *Proc. Nat. Acad. Sci. USA* **98**, 10037.
- Banks, D. S. and Fradin, C.: 2005, Anomalous diffusion of proteins due to molecular crowding, *Biophys. J.* **89**, 2960–2971.
- Bartussek, R., H anggi, P. and Kissner, J. G.: 1994, Periodically rocked thermal ratchets, *EPL (Europhysics Letters)* **28**(7), 459.
- Bruno, L., Levi, V., Brunstein, M. and Desposito, M. A.: 2009, Transition to superdiffusive behavior in intracellular actin-based transport mediated by molecular motors, *Phys. Rev. E* **80**, 011912.
- Bruno, L., Salierno, M., Wetzler, D. E., Desposito, M. A. and Levi, V.: 2011, Mechanical properties of organelles driven by microtubuli-dependent molecular motors in living cells, *PLoS ONE* **6**, e18332.
- Caspi, A., Granek, R. and Elbaum, M.: 2002, Diffusion and directed motion in cellular transport, *Phys. Rev. E* **66**, 011916.
- Cheng, C., McGonigal, P. R., Stoddart, J. F. and Astumian, R. D.: 2015, Design and synthesis of nonequilibrium systems, *ACS Nano* **9**, 8672–8688.
- Doering, C. R., Horsthemke, W. and Riordan, J.: 1994, Nonequilibrium fluctuation-induced transport, *Phys. Rev. Lett.* **72**, 2984–2987.
- Erbas-Cakmak, S., Leigh, D. A., McTernan, C. T. and Nussbaumer, A. L.: 2015, Artificial molecular machines, *Chem. Rev.* **115**, 10081–10206.
- Gittes, F., Schnurr, B., Olmsted, P. D., MacKintosh, F. C. and Schmidt, C. F.: 1997, Microscopic viscoelasticity: Shear moduli of soft materials determined from thermal fluctuations, *Phys. Rev. Lett.* **79**, 3286–3289.
- Golding, I. and Cox, E. C.: 2006, Physical nature of bacterial cytoplasm, *Phys. Rev. Lett.* **96**, 098102.
- Gorenflo, R. and Mainardi, F.: 1997, in A. Carpinteri and F. Mainardi (eds), *Fractal and Fractal Calculus in Continuum Mechanics*, Springer, Wien, pp. 223–276.
- Goychuk, I.: 2009, Viscoelastic subdiffusion: from anomalous to normal, *Phys. Rev. E* **80**, 046125.
- Goychuk, I.: 2010, Subdiffusive brownian ratchets rocked by a periodic force, *Chem. Phys.* **375**, 450–457.
- Goychuk, I.: 2012a, Fractional time random walk subdiffusion and anomalous transport with finite mean residence times: faster, not slower, *Phys. Rev. E* **86**, 021113.
- Goychuk, I.: 2012b, Viscoelastic subdiffusion: Generalized langevin equation approach, *Adv. Chem. Phys.* **50**, 187–253.
- Goychuk, I.: 2015, Anomalous transport of subdiffusing cargos by single kinesin motors: the role of mechanochemical coupling and anharmonicity of tether, *Phys. Biol.* **12**, 016013.
- Goychuk, I.: 2016, Molecular machines operating on the nanoscale: from classical to quantum, *Beilstein J. Nanotechnol.* **7**, 328–350.
- Goychuk, I.: 2017, Viscoelastic subdiffusion in random gaussian potentials, *arXiv:1712.05238 [cond-mat.stat-mech]*.
- Goychuk, I. and Kharchenko, V.: 2012, Fractional brownian motors and stochastic resonance, *Phys. Rev. E* **85**, 051131.
- Goychuk, I. and Kharchenko, V. O.: 2013, Rocking subdiffusive ratchets: origin, optimization and efficiency, *Math. Model. Nat. Phenom.* **8**, 144–158.
- Goychuk, I., Kharchenko, V. O. and Metzler, R.: 2014a, How molecular motors work in the crowded environment of living cells: Coexistence and efficiency of normal and anomalous transport, *PLoS ONE* **9**, e91700.
- Goychuk, I., Kharchenko, V. O. and Metzler, R.: 2014b, Molecular motors pulling cargos in the viscoelastic cytosol: how power strokes beat subdiffusion, *Phys. Chem. Chem. Phys.* **16**, 16524.
- Guigas, G., Kalla, C. and Weiss, M.: 2007, Probing the nanoscale viscoelasticity of intracellular fluids in living cells, *Biophys. J.* **93**, 316.
- Harrison, A. W., Kenwright, D. A., Waigh, T. A., Woodman, P. G. and Allan, V. J.: 2013, Modes of correlated angular motion in live cells across three distinct time scales, *Phys. Biol.* **10**, 036002.
- Herrchen, M. and  ottinger, H. C.: 1997, A detailed comparison of various fene dumbbell models, *J. Non-Newtonian Fluid Mech.* **68**, 17.
- Hill, T. L.: 1989, *Free Energy Transduction and Biochemical Cycle Kinetics*, Springer, New York.
- Hirokawa, N. and Takemura, T.: 2005, Molecular motors and mechanisms of directional transport in neurons, *Nature Reviews* **6**, 201–214.
- Hughes, B. D.: 1995, *Random Walks and Random Environments*, Clarendon Press, Oxford.
- Jeon, J.-H., Monne, H. M.-S., Javanainen, M. and Metzler, R.: 2012, Anomalous diffusion of phospholipids and cholesterol in a lipid bilayer and its origins, *Phys. Rev. Lett.* **109**, 188103.
- Jeon, J. H., Tejedor, V., Burov, S., Barkai, E., Selhuber-Unkel, C., Berg-S orensen, K., Oddershede, L. and Metzler, R.: 2011, In vivo anomalous diffusion and weak ergodicity breaking of lipid granules, *Phys. Rev. Lett.* **106**, 048103.
- J licher, F., Ajdari, A. and Prost, J.: 1997, Modeling molecular motors, *Rev. Mod. Phys.* **69**, 1269.
- Kharchenko, V. O. and Goychuk, I.: 2012, Flashing subdiffusive ratchets in viscoelastic media, *New J. Phys.* **14**, 043042.
- Kharchenko, V. O. and Goychuk, I.: 2013, Subdiffusive rocking ratchets in viscoelastic media: Transport optimization and thermodynamic efficiency in overdamped regime, *Phys. Rev. E* **87**, 052119.

- Kneller, G. R., Baczynski, K. and Pasenkiewicz-Gierula, M.: 2011, Communication: Consistent picture of lateral subdiffusion in lipid bilayers: Molecular dynamics simulation and exact results, *J. Chem. Phys.* **135**, 141105.
- Kojima, H., Muto, E., Higuchi, H. and Yanagida, T.: 1996, Mechanics of single kinesin molecules measured by optical trapping nanometry, *Biophys. J.* **73**, 2012.
- Kolmogorov, A. N.: 1940, Wiener spirals and some other interesting curves in a hilbert space, *Dokl. Akad. Nauk SSSR* **26**, 115–118 (in Russian).
- Kolmogorov, A. N.: 1991, Wiener spirals and some other interesting curves in a hilbert space, in V. M. Tikhomirov (ed.), *Selected Works of A. N. Kolmogorov, vol. I, Mechanics and Mathematics*, Kluwer, Dordrecht, pp. 303–307.
- Kubo, R.: 1966, Fluctuation-dissipation theorem, *Rep. Prog. Theor. Phys.* **29**, 255.
- Larson, R. G.: 1999, *The Structure and Rheology of Complex Fluids*, Oxford University Press, New York.
- Luby-Phelps, K.: 2013, The physical chemistry of cytoplasm and its influence on cell function: an update, *Mol. Biol. Cell* **24**, 2593.
- Magnasco, M. O.: 1993, Forced thermal ratchets, *Phys. Rev. Lett.* **71**, 1477–1481.
- Makhnovskii, Y. A., Rozenbaum, V. M., Yang, D.-Y., Lin, S. H. and Tsong, T. Y.: 2004, Flashing ratchet model with high efficiency, *Phys. Rev. E* **69**, 021102.
- Mandelbrot, B. and van Ness, J.: 1968, Fractional brownian motion, fractional gaussian noise and applications, *SIAM Rev.* **10**, 422.
- Mason, T. G. and Weitz, D. A.: 1995, Optical measurements of frequency-dependent linear viscoelastic moduli of complex fluids, *Phys. Rev. Lett.* **74**, 1250–1253.
- Mathai, A. M. and Haubold, H. J.: 2017, *An Introduction to Fractional Calculus*, Nova Science Publishers, New York.
- Nelson, P.: 2003, *Biological Physics: Energy, Information, Life*, W. H. Freeman, New York.
- Palmer, R. G., Stein, D. L., Abrahams, E. and Anderson, P. W.: 1984, Models of hierarchically constrained dynamics for glassy relaxation, *Phys. Rev. Lett.* **53**, 958–961.
- Pan, W., Filobelo, L., Pham, N. D. Q., Galkin, O., Uzunova, V. V. and Vekilov, P. G.: 2009, Viscoelasticity in homogeneous protein solutions, *Phys. Rev. Lett.* **102**, 058101.
- Parmeggiani, A., Jülicher, F., Ajdari, A. and Prost, J.: 1999, Energy transduction of isothermal ratchets: Generic aspects and specific examples close to and far from equilibrium, *Rev. Rev. E* **60**, 2127.
- Phillips, R., Kondev, J., Theriot, J. and Garcia, H. G.: 2013, *Physical Biology of the Cell*, 2nd edn, Garland Science, London.
- Pollard, T. D., Earnshaw, W. C. and Lippincott-Schwarz, J.: 2008, *Cell Biology*, 2nd edn, Saunders Elsevier, Philadelphia.
- Prost, J., Chauwin, J.-F. m. c., Peliti, L. and Ajdari, A.: 1994, Asymmetric pumping of particles, *Phys. Rev. Lett.* **72**, 2652–2655.
- Qian, H.: 2005, Cycle kinetics, steady state thermodynamics and motors – a paradigm for living matter physics, *J. Phys. Cond. Matt.* **17**, S3783–S3794.
- Reimann, P.: 2002, Brownian motors: noisy transport far from equilibrium, *Phys. Rep.* **361**, 57–265.
- Robert, D., Nguyen, T.-H., Gallet, F. and Wilhelm, C.: 2010, Diffusion and directed motion in cellular transport, *PLoS ONE* **4**, e10046.
- Rousselet, J., Salome, L., Ajdari, A. and Prost, J.: 1994, Directional motion of brownian particles induced by a periodic asymmetric potential, *Nature (London)* **370**, 446.
- Rozenbaum, V. M., Yang, D.-Y., Lin, S. H. and Tsong, T. Y.: 2004, Catalytic wheel as a brownian motor, *J. Phys. Chem. B* **108**, 15880–15889.
- Santamaría-Holek, I., Rubí, J. M. and Gadowski, A.: 2007, Thermokinetic approach of single particles and clusters involving anomalous diffusion under viscoelastic response, *J. Phys. Chem. B* **111**, 2293–2298.
- Saxton, M. J. and Jacobson, K.: 1997, Single-particle tracking: applications to membrane dynamics, *Annu. Rev. Biophys. Biomol. Struct.* **26**, 373.
- Seisenberger, G., Ried, M. U., Endress, T., Büning, H., Hallek, M. and Bräuchle, C.: 2001, Real-time single-molecule imaging of the infection pathway of an adeno-associated virus, *Science* **294**, 1929–1932.
- Svoboda, K., Schmidt, C. F., Schnapp, B. J. and Block, S. M.: 1993, Direct observation of kinesin stepping by optical trapping interferometry, *Nature (London)* **365**, 721–727.
- Tabei, S. M. A., Burov, S., Kima, H. Y., Kuznetsov, A., Huynh, T., Jureller, J., Philipson, L. H., Dinner, A. R. and Scherer, N. F.: 2013, Intracellular transport of insulin granules is a subordinated random walk, *Proc. Natl. Acad. Sci. (USA)* **110**, 4911–4916.
- Tolic-Norrelykke, I. M., Munteanu, E.-L., Thon, G., Oddershede, L. and Berg-Sorensen, K.: 2004, Anomalous diffusion in living yeast cells, *Phys. Rev. Lett.* **93**, 078102.
- Waigh, T. A.: 2005, Microrheology of complex fluids, *Rep. Progr. Phys.* **68**, 685.
- Weigel, A. V., Simon, B., Tamkun, M. M. and Krapf, D.: 2011, Ergodic and nonergodic processes coexist in the plasma membrane as observed by single-molecule tracking, *Proc. Natl. Acad. Sci. (USA)* **108**, 6438–6443.
- Weiss, M.: 2013, Single-particle tracking data reveal anticorrelated fractional brownian motion in crowded fluids, *Phys. Rev. E* **88**, 010101.
- Weiss, M., Elsner, M., Kartberg, F. and Nilsson, T.: 2004, Anomalous subdiffusion is a measure for cytoplasmic crowding in living cells, *Biophys. J.* **87**, 3518–3524.
- Weiss, U.: 1999, *Quantum Dissipative Systems*, 2nd edn, World Scientific, Singapore.
- Wyman, J.: 1975, The turning wheel: a study in steady states, *Proc. Nat. Acad. Sci. USA* **72**, 3983.
- Zwanzig, R.: 2001, *Nonequilibrium Statistical Mechanics*, Oxford University Press, Oxford.

